Charge Density in the $[Mo(NCS)_6]^{3-}$ Ion in $Cs_3Mo(NCS)_6$†

Christopher D. Delfs, Brian N. Figgis,* Edward S. Kucharski, and Philip A. Reynolds
School of Chemistry, University of Western Australia, Nedlands, W.A. 6009, Australia

High-quality *X*-ray data sets were collected on the new and simple molybdenum(III) complex $Cs_3Mo(NCS)_6$ at 295 and 115 K. The 1 102 unique data at 115 K were analysed using a multipole model of the charge density to give $R(I)$ 0.015, χ^2 1.38. The structure consists of $[Mo(NCS)_6]^{3-}$ octahedra compressed down a three-fold axis along *c*. There is disorder over the two equivalent rotations of the octahedron about *c*. Deformation density maps show strong peaks at the Cs and Mo positions which probably arise from the disorder and/or anharmonic thermal motion. A valence-orbital analysis of the data restricted to $(\sin\theta)/\lambda < 7$ nm^{-1} because of the disorder/anharmonicity is able to define the covalent charge transfers to and from the Mo atom and within it, the NCS group, and the Cs atoms. The Mo configuration is $4d^{2.5(3)}5(s/p)^{2.0(4)}$, with a strong contraction of the 4*d* radius, to about 2/3 of the free-ion value. The high diffuse population and 4*d* orbital contraction are believed to reflect high covalence in the bonding to the NCS^- ion, which has comparable σ-donation and π-back-bonding components. The electronic structure of the NCS^- ion is well defined and shows good agreement with an *ab initio* calculation. The magnetic susceptibility of the compound shows evidence of substantial magnetic exchange [$\theta = -20.1(1)$ K] and a pathway for this is provided by the close intermolecular S ··· S contacts.

Charge and spin-density studies of transition-metal complexes have largely been applied to compounds of the first-row elements because of their better defined and more ionic chemistry, and the smaller number of core electrons relative to the second and third series. However, those heavier transition metals have a rich and important chemistry in which covalent effects are more obvious than for the first series.

We wish to extend the application of spin-density studies to bonding in the complexes of the heavier transition metals, employing the technique of polarised neutron diffraction (p.n.d.). For experimental reasons it is very desirable to use complexes of spin $S > \frac{1}{2}$. Such complexes are rare for the second and third transition-series metals, the only well known examples being for the d^3 configurations present in Mo^{III} and Re^{IV}, in octahedral co-ordination. A p.n.d. study of K_2ReCl_6 has been reported [1] but has not been fully analysed because of problems with structural details. We looked for molybdenum(III) complexes of simple structure which might be available in the form of the large single crystals required for the p.n.d. experiment. The structure of a solvated salt has been reported but the complex structure is unsuitable for our purposes.[2]

A chromium complex $K_3Cr(SCN)_6\cdot 4H_2O$ is known,[3] and the use of heavier alkali-metal counter ions often reduces the hydration of crystalline salts, and also often gives a well defined crystal system. We readily obtained $Cs_3Mo(NCS)_6$ and found that large crystals can be grown. As we shall see, $Cs_3Mo(NCS)_6$ has a particularly simple and symmetrical crystal structure containing the $[Mo(NCS)_6]^{3-}$ ion. Investigation of the magnetic susceptibility of the compound indicates that there appears to be appreciable magnetic exchange present, so that there may not be sufficient magnetisation available at the usual temperature and magnetic field of the p.n.d. experiment to give satisfactory results. However, the compound, because of its particularly simple crystal structure, is a highly attractive proposition for a charge-density study of the bonding present. That aspect is dealt with in this paper.

Previous charge-density studies on the caesium-containing compounds $Cs_2KCr(CN)_6$,[4] Cs_2CoCl_4,[5] Cs_3CoCl_5,[6] and on some second transition series compounds, for example $[Mo_2(CH_3CO_2)_4]$ [7] and $[Ru_3H_3(CO)_9CCl]$,[8] have shown that useful information concerning the valence-electron density distribution of the transition-metal ion can be obtained even though there are large numbers of core electrons present in the unit cell. Particularly useful for comparison of bonding in light and heavy metals are studies of the charge density in $[Cr(CN)_6]^{3-}$ and the spin densities in that ion [9,10] and in the $[CrF_6]^{3-}$ ion.[11,12]

In this paper we present the experimental procedure followed by a least-squares analysis of the data in terms of a multipole expansion of the density, and, alternatively, in terms of valence-orbital populations. The charge-density results are then discussed with reference to other charge-density and to spin-density studies on chromium(III) complexes. In a later paper we shall present calculations, using the *ab initio* DV-Xα method, of the charge and spin densities in the $[Mo(NCS)_6]^{3-}$ ion, and compare them with the present experimental results.

Experimental

Crystal Preparation.—The salt $[NH_4]_3[Mo(NCS)_6]\cdot 6H_2O$ was prepared by a standard method.[13] A concentrated aqueous solution of it was mixed with a saturated solution of CsCl, in a stoicheiometric amount, in an inert atmosphere. The precipitate of $Cs_3Mo(NCS)_6$ was collected and dried *in vacuo*. Slow evaporation of a saturated aqueous solution of the compound in an inert atmosphere yielded large amber crystals, typically in the form of elongated hexagonal rods with (001) a pronounced cleavage plane. Many of the crystals showed darker regions in planes parallel to (001). Analysis confirmed the formulation [Found: Mo, 11.60; S, 22.70. Calc. for $Cs_3Mo(NCS)_6$: Mo, 11.40; S, 22.80%].

Magnetic Susceptibility.—The magnetic susceptibility of a powdered specimen of $Cs_3Mo(NCS)_6$ was measured at 14 temperatures between 80 and 230 K on equipment previously described.[14] The Curie–Weiss law [equation (1)] was found

† *Supplementary data available:* see Instructions for Authors, *J. Chem. Soc., Dalton Trans.*, 1989, Issue 1, pp. xvii—xx.

Table 1. Crystal data and experimental conditions for $Cs_3Mo(NCS)_6$

M_r	843.1		
Space group	*P6/mmm*		
T/K	295(2)		115(4)
a/nm	1.097 0(3)		1.094 9(3)
c/nm	0.500 8(2)		0.494 9(2)
U/nm^3	0.521 9(4)		0.513 8(3)
Z	1		
$D_{obs.}$/g cm^{-3}	2.61(1)		
$D_{calc.}$/g cm^{-3}	2.682		2.725
μ/mm^{-1}	6.00		6.09
λ(Mo-K_α)/pm	71.069		
F(000)	378.1		
$2\theta_{max.}$/°	100		
Max.(sin θ)/(nm^{-1})	10.79		
Scan mode, angle/°	ω—2θ, 1.95 plus α_1—α_2 splitting		
Monochromator	Graphite plate		
Background	0.5 scan time		
Standards	8 per 100 reflections		
Crystal dimensions,	(001)	180	203
from arbitrary	(00 − 1)	180	203
centre/μm	(100)	52	59
	(−100)	52	59
	(010)	53	56
	(0 − 10)	53	56
	(1 − 10)	50	59
	(−110)	50	59
Transmission factor	0.496—0.597		0.447—0.562
Reflections measured	12 312		29 190
Merging R_1	0.018		0.015
Unique reflections	1 131		1 102

Table 2. Refinements of the reflection data for $Cs_3Mo(NCS)_6$

	Spherical theoretical atom		Aspherical, 115 K	
	295 K	115 K	Multipole	Valence
Max.(sin θ)/λ (nm^{-1})	10.8	10.8	10.8	7.0
No. of reflections	1 131	1 102	1 102	329
No. with $I > 3\sigma(I)$	861	863	863	314
No. of variables	28	28	72	30
χ^2	2.81	2.56	1.38	1.56
$R(I)$	0.030	0.025	0.015	0.013
R'	0.074	0.053	0.028	0.022
$R(F)$, $I > 3\sigma(I)$	0.033	0.019	0.013	0.008

Table 3. Positional parameters for $Cs_3Mo(NCS)_6$ ($\times 10^4$); first entry 295 K, second entry 115 K, using spherical atoms, third entry 115 K full multipole refinement

Atom	x	y	z
Mo	0	0	0
Cs	5 000	0	0
N	1 846(3)	$=x/2$	2 263(5)
	1 856(2)		2 277(4)
	1 862(1)		2 283(3)
C	2 930(3)	$=x/2$	3 344(7)
	2 947(2)		3 375(4)
	2 952(1)		3 377(3)
S	4 473(1)	$=x/2$	4 803(17)
	4 495(1)		4 882(18)
	4 496(1)		4 892(7)

$$\chi_{Mo} = C(T - \theta)^{-1} \quad (1)$$

to hold, where $C = 22.2(2) \times 10^{-6}$ m^3 K mol^{-1} and $\theta = -20.1(1)$ K.

Data Collection.—Preliminary examination of $Cs_3Mo(NCS)_6$ was by Weissenberg photographic methods. In view of the disorder invoked in the structure solution, this was repeated to include long periods of exposure. No noticeable streaking appeared, but the result is not clear as the background was rather high.

A small hexagonal prism of the compound was mounted on a Syntex $P2_1$ diffractometer at *ca.* 295 K. Eight strong reflections, well separated in angle, were centred and a unit cell was derived by least-squares fitting. The unit cell was hexagonal and the Laue symmetry close to 6/*mmm*. A hemi-sphere of reflection data to $2\theta = 100°$ was collected. The standard reflections showed no systematic variation with time. A second crystal was cooled to 115(4) K by means of a locally developed nitrogen gas flow device, and a further complete sphere of data collected. The crystal and experimental conditions are in Table 1.

Data Processing.—After correction for variation of the standards with time, a correction to the reflection intensities for absorption was made in 6/*mmm* symmetry, using the XTAL[15] suite of programs. Keeping the volume constant at the measured value, the crystal dimensions were used as adjustable parameters to minimise agreement, $\Sigma[I - \text{av}(I)]^2$, between the 24 equivalents of each reflection. The refined dimensions were not significantly different from those measured and the excellent agreement factors obtained (Table 1) confirmed the Laue symmetry of the crystal as 6/*mmm* at both temperatures. Examination of the variation of the standards with time gave an estimate of the instrumental instability as 1%, so the reflection intensities were assigned standard errors derived from the agreement between the equivalents, but augmented by that figure.

Structure Solution and Refinement.—On assuming that $Z = 1$, because of the cell volume, and that the molybdenum atom is octahedrally co-ordinated, *P6/mmm* was found to be the only suitable hexagonal space group. The $\bar{3}m$ site symmetry required the anion to be disordered over two orientations. A less likely option was the trigonal space group $P\bar{3}1m$ with twins of equal volume. Consideration of the ionic radii of the atoms concerned produced a preferred structure with Cs^+ ions on *f* sites and NCS^- ions on *n* sites. Inspection showed that the *h*-even and *k*-even reflections were very intense, confirming the assignment of the Cs^+ ions to the *f* sites. The positions of N, C, and S atoms were then calculated assuming normal bond lengths.

The ambient-temperature and the low-temperature data sets were each refined from the initial starting parameters of the above model, employing only the reflections at low values of θ at first, but finally using all members of the sets, minimising $\Sigma\sigma(I)^{-2}(I_{obs.} - I_{calc.})^2$. Scattering factors for Cs^+, Mo^{3+}, N, C, and S were taken from a standard compilation[16] and modified for anomalous dispersion.[17] The program ASRED[5] was used. The very good final agreement factors obtained (Table 2) confirm the assignment of the space group and the details of the structure. The positional parameters deduced are given in Table 3.

Additional material available from the Cambridge Crystallographic Data Centre comprises thermal parameters.

As in the previous cases of Cs_2CoCl_4[5] and Cs_3CoCl_5,[6] empirical corrections for anisotropic absorption and extinction and for multiple scattering were introduced into the calculated intensities. The use of a Type I anisotropic extinction model yielded, in addition to the isotropic term, only one parameter significant above the errors. The two terms were combined into a small extinction correction of the form $e\cos^2\alpha$, where e is the extinction parameter and α is the angle between the scattering vector, $\vec{K}$, and the *c* crystal axis direction. The largest correction

Table 4. Valence parameters derived from the multipole analysis of the reflection data for $Cs_3Mo(NCS)_6$. Multipoles and estimated standard deviations (e.s.d.s) are given in parentheses

		(00)	(20)	(40)	K_{4d}				
Mo	4*d*	2.3(3)	1.4(4)	−0.2(1)	0.72(8)				
	5*p*	3.0(9)	0.6(5)	−1.5(5)					
		(00)	(20)	(22)	(40)	(42)	(44)	K_{5d}	
Cs	5*d*	10.0*	1.7(5)	0.1(1)	−1.4(1)	0.2(2)	−0.6(2)	1.04(1)	
	6*p*	−1.9(3)	1.3(6)	0.0(2)	−0.7(3)	−0.2(2)	0.1(2)		
	Shell	0.7(2)							
		(00)	(10)	(1 − 1)	(20)	(2 − 1)	(22)	(30)	K_{nsp}
N	2*sp*	5.0(3)	−0.1(1)	−0.1(1)	0.5(1)	0.2(2)	0.0(1)	−0.1(1)	0.99(2)
C	2*sp*	4.7(3)	−0.2(2)	0.0(1)	1.2(2)	−0.2(2)	−0.5(2)	0.3(1)	1.05(2)
S	3*sp*	6.6(1)	1.0(6)	2.5(18)	−1.5(4)	0.2(5)	−1.8(5)	0.2(1)	0.92(2)

* Fixed.

Table 5. Bond lengths (pm) and angles (°) in $Cs_3Mo(NCS)_6$ at 115 K

$Mo(NCS)_6$ octahedron			
Mo–N	209.6(1)	Mo–N–C	175.1(1)
N–C	116.7(2)	N–C–S	179.5(2)
C–S	164.5(2)	N–Mo–N	93.7(1)
Intermolecular contacts			
Mo · · · Mo^{I}	494.9(2)	Cs · · · S^{II}	375.7(3)
Cs · · · S	368.6(2)	S^{II} · · · Cs	375.7(3)
S · · · Cs	368.6(2)	S · · · S^{IV}	356.7(1)
S · · · S^{III}	356.5(1)	S · · · S^{VI}	426.3(1)*
S · · · S^{V}	426.5(1)		

I $x, y, 1 + z$; II $x, y, z - 1$; III $1 - y, 1 - x, z$; IV $1 - y, 1 - x, 1 - z$; V $y, -x, 1 - z$; VI y, x, z*.

* Apparent contact due to disorder, not actually possible, see text.

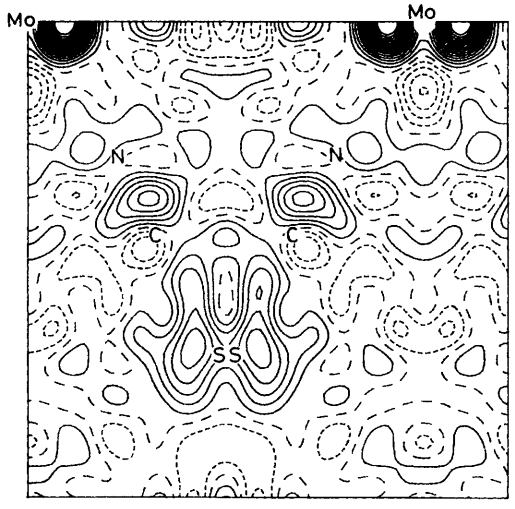

Figure 1. Deformation density in the plane containing the Mo atom and an NCS group. The crystal *c* axis is vertical and the [210] direction is horizontal. Contour intervals are 100 e nm^{-3}, positive (full lines), negative (dotted lines). The plane extends 600 pm from the top left Mo atom in each direction

for any reflection corresponded to a 1.5% decrease in the observed intensity. Two terms were introduced in the multiple scattering correction, which took the form (2). For the data at

$$\vec{I}(\text{obs.}) = I(\text{obs.}) + m_1 + m_2(1 - |\vec{K}|) \qquad (2)$$

115 K the intensity correction varied from only 260(60) counts at $|\vec{K}| = 0$ to 33(11) counts at $|\vec{K}| = 10$ nm^{-1}, relative to 3.7×10^6 counts for the strongest reflection measured.

Refinements

We modelled the electron density in $Cs_3Mo(NCS)_6$ by a set of multipolar density functions, closely following our previous procedures.[4–6] On the molybdenum atom we placed core, 4*d* and 5*p* radial functions; on the caesium atom, core, 5*d* and 6*p* functions, and a thin shell of radius 150 pm from the nucleus; on the sulphur atom, core and 3*p* functions; on the carbon and nitrogen atoms, core and 2*p* functions. The form factors required (j_0 to j_4 as appropriate) for each radial function[4] were calculated from the Hartree–Fock neutral-atom wavefunctions of ref. 18, except for the case of caesium where those of ref. 4 were employed. The angular variations associated with the valence functions were symmetry-adapted sets to order four for caesium and molybdenum, and to order two, augmented by one of order three, for the lighter atoms. The axes for the sets had *z* parallel to the crystal *c* axis and *x* parallel to *a* for caesium and molybdenum, and *z* directed towards Mo and *x* perpendicular to the mirror plane of the $Mo(NCS)_6$ octahedron for nitrogen, carbon, and sulphur. On each atom the radius of the outermost formally occupied function was refined as a variable by using $K_i r$ in place of *r*, where K_i is the variable associated with atom *i*.

This model, with 44 valence-electron variables, was refined constraining the total number of electrons to the formula value. We obtained the agreement factors given in Table 2, the positional values given in Table 3, and the charge density parameters given in Table 4. The close approach of disordered sulphur atoms causes correlation between certain of their parameters, principally *z*, U_{33}, and especially the multipole (1, −1). The errors to be associated with those parameters are correspondingly large. Important features of the $Mo(NCS)_6$ unit geometry and some 'intermolecular' contacts are shown in Table 5. Using the values of the positional, thermal, and other parameters derived in this refinement with data to $|\vec{K}| = 8$ nm^{-1}, and employing neutral spherical-atom scattering factors,[16] we calculated the deformation density for the plane containing the Mo atom, an NCS group, and the crystal *c* axis, which is shown in Figure 1. Similarly, we calculated the deformation density for the $x = \frac{1}{2}$ plane containing four caesium and an almost in-plane central sulphur atom, which is shown in Figure 2. The corresponding residual density maps based upon the refinement multipole model are shown in Figures 3 and 4.

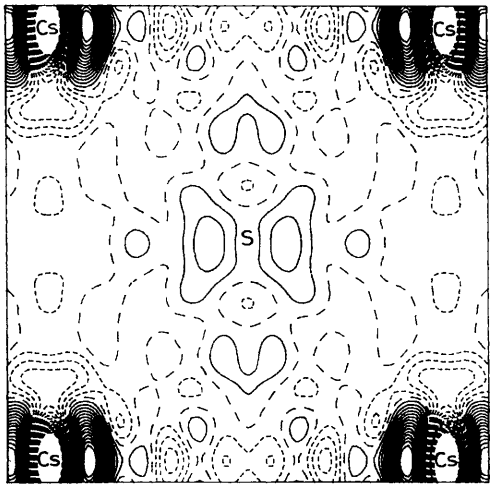

Figure 2. Deformation density in the $x = \frac{1}{2}$ plane, containing Cs atoms and, approximately, S atoms. The crystal c axis is horizontal and the [102] direction is vertical. The plane extends 300 pm each side of the S atom in each direction. Contour intervals are as for Figure 1

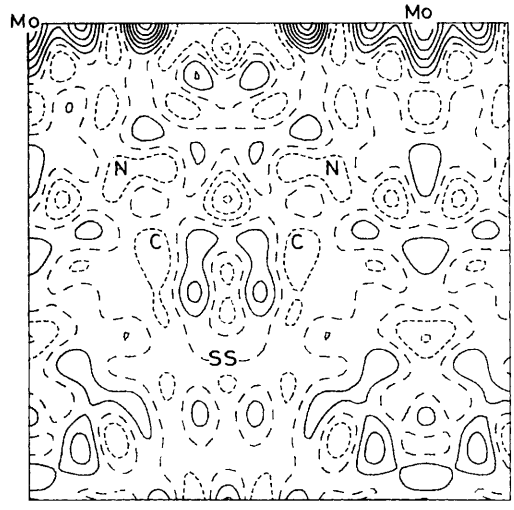

Figure 3. Residual density from the multipole fit of the data, in the Mo–NCS plane. Specifications are as for Figure 1

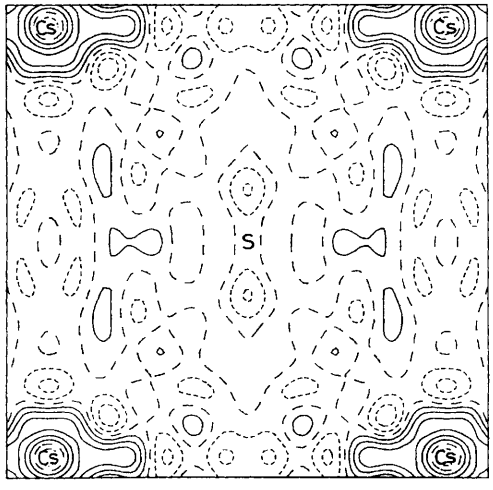

Figure 4. Residual density from the multipole fit to the data in the Cs–S plane. Specifications are as for Figure 2

Many of the parameters in the above multipole model appear to be redundant. For example, some of the multipoles in the valence shells of each of the heavy atoms are not defined at a good level of significance. They, and the variable valence function radii, were introduced after other studies[4–6,19] showed their importance for more highly polarisable atoms. Similarly, a relatively large number of valence functions on the light atoms were used because 'intermolecular' polarisation of light-atom ligands has been observed elsewhere.[4] It is very likely that almost as good a fit can be obtained with a simpler model. However, the full multipole refinement is an invaluable guide to the nature of such models. Without it a simple model might produce unrealistically small standard errors for parameters which were not well designed to describe density.

A particularly relevant point is the behaviour of the (2, 0) and (4, 0) multipoles of the molybdenum atom. A refinement of data within thin shells of $(\sin\theta)/\lambda$ shows that for $|\underline{K}| < 7$—8 nm^{-1} the form factors j_0, j_2, and j_4 correspond well to those expected for a distribution arising from 4d electrons. At higher values of $|\underline{K}|$ the observed value of j_4 changes sign from that expected from the low-angle data on the basis of 4d electrons. The two-variable radius treatment of the full multipole model can accommodate such a feature but the high-angle data, apparently depending on a source other than 4d electrons, severely bias an estimate of the 4d population. The caesium atom is also distorted from spherical symmetry in a similar fashion. In order to allow a better estimate of 4d orbital population we decided to restrict data to $|\underline{K}| < 7$ nm^{-1} in further refinements.

We performed a refinement in which we refined populations of suitable hybrid orbitals in the valence region in place of multipoles. The positional, thermal, and other parameters were kept fixed at the values deduced in the full multipole treatment. In the light of the multipole model results the Cs, N, C, and S atoms were constrained to have cylindrical symmetry about their z axis. Guided by the deformation density maps, the z axis of the S atom was defined to be along the (210) direction and the x axis along c. For each of the S, C, and N atoms we employed (sp) hybrid orbitals, with $(sp)_1$ along z and $(sp)_2$ along $-z$. The labelling of the valence functions is otherwise self-explanatory, except for 4d orbitals of the molybdenum atom. In the $\bar{3}m$ site symmetry of that atom the 4d orbitals split into three sets; the σ-bonding 4d-e (e_σ), the π-bonding 4d-e (e_π), and the $4d_{z^2}$ (a_1) orbital. The agreement factors obtained for the refinement are given in Table 2.

Deformation density maps show very strong peaks at the caesium positions, as well as at other positions. We modelled these peaks by valence-electron populations, with fixed caesium orbital radii, and, alternatively, by changing the Cs–5d radial parameter but not the population. From the point of view of theory the second procedure is probably the more attractive picture of polarisation. We obtained very similar fits: the Cs–5d radial parameters and populations are highly correlated. For the radial variation model the values of $\underline{K}_{Cs}$ obtained were: $5d_{xz,yz}$, 1.28(50); $5d_{xy,x^2-y^2}$, 0.97(7); and $5d_{z^2}$, 0.76(9). These radial changes, or, equivalently, the population changes, were much larger than we expected for valence-electron polarisation in the light of previous studies. To clarify this matter we investigated a number of models for the caesium site involving anharmonic thermal motion and disorder and with the caesium scattering centre constrained to spherical symmetry. The introduction of $|\underline{K}|^n$, $n = 3$ or 4, anharmonic thermal motion terms produced little improvement in the fit. A single extra caesium atom at $\frac{1}{2}$, 0, z, with occupation and z refined, yielded a population of 0.010 6(7) times that of the $\frac{1}{2}$, 0, 0 site at $z = 0.114(5)$. The fit was improved, but the value of χ^2 did not approach that of the multipole model. Other manipulations of the Cs site to smear

Table 6. Valence-orbital populations in $Cs_3Mo(NCS)_6$. For Mo the nomenclature is for point group D_3, the site symmetry, although each of the ions contributing to the disorder belongs to the group D_{3h}. The orbitals e_σ, e_π, and a_1 are combinations of the d_{xz}, d_{yz}, d_{xy}, $d_{x^2-y^2}$, and d_{z^2} orbitals as discussed in B. N. Figgis and P. A. Reynolds, *Inorg. Chem.*, 1985, **24**, 1864. For Cs the nomenclature is for the point group D_{2d} and the labelling of the e orbitals is arbitrary

Mo	4*d*	e_σ	1.3(5)	e_π	0.6(5)	a_1	0.6(1)	K_{4d}	0.67(9)
	5*p*	*e*	1.6(6)	a_1	0.4(4)				
Cs	5*d*	e_α	5.6(2)	e_β	3.6(2)	a_1	1.6(2)	K_{5d}	1.07(1)
	6*p*	*e*	−0.9(2)	a_1	−0.8(3)				
	Shell		0.2(3)						
N	2*sp*	$(sp)_1$	1.8(1)	$(sp)_2$	1.9(1)	p_π	2.0(1)	K_{2sp}	1.04(1)
C	2*sp*	$(sp)_1$	1.5(1)	$(sp)_2$	1.8(1)	p_π	0.8(1)	K_{2sp}	1.00(2)
S	3*sp*	$(sp)_1$	1.0(1)	$(sp)_2$	1.1(1)	p_x	2.3(1)		
						p_y	1.9(1)	K_{3sp}	0.71(3)

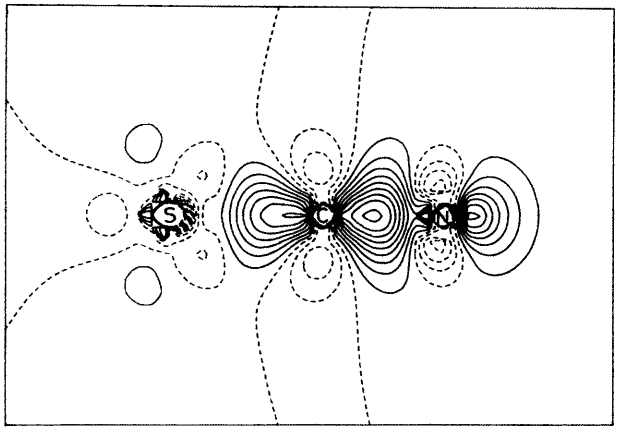

Figure 5. The deformation density of the NCS^- ion from an *ab initio* Hartree–Fock calculation [20]

density along *z* gave only very small further improvements in the fit.

Discussion

Structure.—The crystal structure of $Cs_3Mo(NCS)_6$ is very simple: $Mo(NCS)_6$ octahedra are stacked one above the other with an octahedral three-fold axis along the crystal *c* axis. The sulphur atoms in each such stack are linked to the next stack by interaction with caesium atoms. The octahedra in a stack can occupy one of two orientations related by a rotation of 60° about the *c* axis. This rotation causes little alteration to the interstack Cs–S contact distances but strong interference within the stack.

The geometry of the $[Mo(NCS)_6]^{3-}$ unit is much as expected from the only previous study of the ion, in $K_3Mo(NCS)_6 \cdot H_2O \cdot CH_3CO_2H$.[3] The present results are much more precise. The octahedron is distorted along the crystal *c* axis, the N–Mo–N angle opening from 90 to 93.7(1)°. The C and S atom positions are moved relatively further from ideal positions so that, while the NCS unit remains linear [N–C–S angle 179.5(2)°] the Mo–N–C angle decreases to 175.1(1)°. The resulting *z* co-ordinate of the S atom is very close to 0.5 so that, irrespective of the $Mo(NCS)_6$ stack disorder, the remaining contacts are little altered. Each S atom has nine neighbours: four caesium atoms arranged in a rectangle in the $x - \frac{1}{2}$ plane; the C atom; two sulphur atoms, close and on the far side from C; and a further two sulphur atoms, more distant on the same side as C. Each Cs atom has eight sulphur atom neighbours, arranged in a cube tetragonally compressed along *a*.

The angular variation in extinction, the slightly low observed density, the (001) cleavage plane, and the observed darker regions in that plane are probably connected to the defects required to accommodate the rotational disorder. Rotation of a whole chain of $Mo(NCS)_6$ units by 60° about the crystal *c* axis to cause disorder gives no new, very short, energetically unfavourable contacts in the crystal. In contrast, rotation of a single $[Mo(NCS)_6]^{3-}$ anion within a stack causes severe interference with the neighbours along *c*. The implication is that correlation of $Mo(NCS)_6$ orientations may be much higher along *c* than in the *ab* plane, explaining the observed anisotropy in the extinction. However, the long-exposure Weissenberg photographs did not show the diffuse planar features expected from that correlated disorder. In view of the high background the conclusions cannot be definite, but it seems that further experimentation of a different nature would be required to define the mechanism for the disorder in detail.

Electronic Structure.—The deformation density maps of Figures 1 and 2 show strong features above and below the Cs, Mo, and S atoms. While it is possible that these are electronic polarisation features, the shift in electron density (Table 6) is so large that this seems unlikely. More probably, they are connected with the disorder and/or anharmonicity in the nuclear position vibrations. Unfortunately, although we tested a number of models, we found no good simple description of the features in those terms. The Cs density can be described approximately as a sharp, relatively harmonic, component superimposed on a small diffuse density (*ca.* 1% of the total) extending ±50 pm along *z*. Similar features, but of different symmetry, have been found in Cs_2CoCl_4 [5] and Cs_3CoCl_5.[6] In the latter case they seemed to be connected with the known phase transition. Only an accurate neutron diffraction study of the structure at 115 K could enable a distinction between the alternatives of disorder/anharmonicity and electronic polarisation.

Covalence effects may be seen in the maps of Figure 1, where an excess of density along the NCS unit appears in the nitrogen lone pair, the C–N bond, and the C–S bond regions. We can compare this pattern with the similar arrangement in the maps produced by a good quality Hartree–Fock calculation on the NCS^- ion [20] (Figure 5). The highest observed peak, 500 e nm^{-3}, in the C–N bond, compares with 900 e nm^{-3} in the calculation. The observed peak will have been reduced by thermal smearing while the calculated value is probably too high by about 100 e nm^{-3} because of the neglect of electron–electron correlation. The negative troughs at the C and N sites, perpendicular to the bond axis, also occur in both the observed and the calculated deformation densities. The fact that the peaks in the observed map are not closely centred on the bond axis may not be experimentally significant.

Quantitative estimates of the covalence features can be obtained from the results of the least-squares refinements. The valence orbital refinement gives net atomic charges of −1.7(3) for Cs, +1.5(3) for Mo, −0.7(2) for N, −0.3(1) for C, and −0.3(1) for S. The multipole refinement yields similar values. In particular, we notice that the Cs atom charge is greater than unity while the net NCS group charge is −1.3(3). The division of the total charge into atomic components by the least-squares process of the refinements is somewhat arbitrary, although the populations usually resemble the equally arbitrary numbers obtained by the conventional Mulliken population analysis procedure of theoretical chemistry. The apparent Cs atom charge indicates a significant charge density change due to interaction between that atom and, presumably, the S atoms of NCS groups. Most of the Cs charge increase comes from the very diffuse 6*s*/*p* region where overlap with other atoms should be significant. The substantial changes in Cs atom form factors which accompany such charge movement have already been noted and discussed in more detail for the cases of Cs_2CoCl_4 [5] and Cs_3CoCl_5.[6] There also, diffuse valence-orbital populations are reduced and the shell populations are positive.

The NCS group distribution tells us little that is new. It is affected by interaction with both the Mo and the Cs atoms, and the strong intramolecular bonding prevents a division into σ- and π-population components, since this bonding can alter the σ and π radii differentially.[21]

The charge on the Mo atom is more revealing. The net charge of +1.5(3) e indicates that, relative to the formal Mo^{3+} ion, a net covalent transfer of 1.5 e occurs from the NCS group. However, the Mo atom configuration is $4d^{2.5(3)}5(s/p)^{2.0(4)}$, indicating that the 4*d* shell loses 0.5(3) e while the diffuse 5(*s*/*p*) shell gains 2.0(4) e. The 4*d* shell also contracts markedly in radius. A division into σ and π effects can be obtained by examining the 4*d* populations e_σ1.3(5) and e_π1.2(4) e. The errors on these populations probably do not adequately reflect the systematic errors inherent in the Mo atom populations due to the disorder and/or anharmonicity described above. However, the populations do produce a coherent picture in which the Mo atom accepts charge by σ interaction with the NCS^- ion and π back-donates rather more to that ion and into its own diffuse 5(*s*/*p*) region. The large contraction of the 4*d* radius is also characteristic of strong covalent bonding.[21]

We can compare these large changes in atomic orbital populations and radii to the results for the first-row transition-metal complex ion $[Cr(CN)_6]^{3-}$. The figures we quote are the averages over the three compounds studied,[4] amongst which there is quite reasonable agreement. We might expect the CN^- ligand to produce much stronger effects than the pseudo-halide NCS^-, particularly when the latter is N-bound. However, the charge transfers are only 1.0(4) for σ donation to Cr–3d_σ, 0.5(2) for π back donation from Cr to CN^-, and 0.3(3) e from 3*d* to 4(*s*/*p*) within the Cr atom, accompanied by a 3% contraction in the 3*d* radius. It seems that the change to a second-row transition metal has almost doubled the covalent effects observed, even though the new ligand should cause a movement in the opposite direction. The spin-density results available on some of the chromium(III) complexes mentioned [19] are not directly relevant to the present argument because of the large spin-polarisation effects arising from electron–electron correlation. However, they do indicate that π back donation is as important as σ donation in the metal–ligand bonding covalence effects.

Magnetic Susceptibility.—The variation of the magnetic susceptibility with temperature indicates the presence of magnetic exchange. Other mechanisms for perturbing the magnetic properties for the $^4A_{2g}$ ground term of the formal Mo^{3+} ion from Curie law behaviour, such as zero-field splitting arising from the reduction of symmetry below octahedral, are less likely to produce an effect of the required magnitude. The close S · · · S contacts which occur between adjacent $Mo(NCS)_6$ octahedra down the stacks provide an obvious pathway for the exchange, although the magnitude is perhaps surprisingly high considering the number of intermediate ligand atoms between any adjacent pair of Mo atoms.

Conclusions

We have prepared a trivalent molybdenum complex of exceedingly simple structure and well adapted for study by various physical measurements. We have determined the structure by *X*-ray diffraction with high accuracy at 295 and 115 K and the magnetic susceptibility down to 90 K. Questions remain as to the role of disorder and anharmonicity in the structure and the mechanism of the magnetic exchange present.

We have modelled the charge density by multipole and valence-orbital refinements. The major feature of the deformation density map is a charge polarisation of the Cs, Mo, and S atoms along the crystal *c* axis. A comparison with a neutron diffraction structure would be necessary to characterise the feature as due to true, unexpectedly large, electronic polarisation on the one hand or, more likely, disorder and/or anharmonic effects on the other.

The map also clearly shows deformation density features present in the *ab initio* calculation for the NCS^- ion; *i.e.* N lone pair, N–C, and C–S bonding peaks, and depletion at the N and C atoms perpendicular to the NCS bond axis.

The results of the charge-density refinements indicate a significant interaction between the Cs and the S atoms which perturbs the Cs density significantly from that of the the free Cs^+ ion. The electron distribution around the Mo atom shows that the Mo–NCS covalence effects are much stronger than for comparable first-row transition series cases. We observe both σ bonding and π back bonding charge transfers of *ca.* 1.5 e each, a large (2e) accumulation of charge in diffuse molybdenum-centred orbitals, and a marked contraction of the 4*d* orbital radius. Comparably large effects have only been seen in the charge-density analysis [21] of (phthalocyaninato)cobalt(II), where the ligand is recognised as producing great covalence in the bonding.

In a later paper we shall present an *ab initio* approximate calculation of the bonding in the $[Mo(NCS)_6]^{3-}$ ion and its differences from that in the $[Cr(NCS)_6]^{3-}$ ion, and further discuss the present results.

Acknowledgements

We thank the Crystallography Centre of the University of Western Australia for access to the Syntex P21 diffractometer, Associate Professor A. H. White for help with the data collection, and the Australian Research Grants Scheme for financial assistance.

References

1 P. J. Brown and J. B. Forsyth, *At. Energy Rev.*, 1979, **17**, 345.
2 J. R. Knox and E. Eriks, *Inorg. Chem.*, 1968, **7**, 84.
3 G. S. Zhadanov, Z. V. Zvonkova, and V. P. Glushkova, *Zh. Fiz. Khim.*, 1953, **27**, 106.
4 B. N. Figgis and P. A. Reynolds, *J. Chem. Soc., Dalton Trans.*, 1987 1747.
5 B. N. Figgis, P. A. Reynolds, and A. H. White, *J. Chem. Soc., Dalto Trans.*, 1987, 1737.
6 B. N. Figgis, E. S. Kucharski, and P. A. Reynolds, *Acta Crystallog Sect. B*, in the press.
7 K. Hino, Y. Saito, and M. Bernard, *Acta Crystallogr., Sect. B*, 19 **37**, 2164.

8 N. J. Zhu, C. Lecomte, P. Coppens, and J. B. Keister, *Acta Crystallogr., Sect. B*, 1982, **38**, 1286.
9 B. N. Figgis, J. B. Forsyth, R. Mason, and P. A. Reynolds, *Chem. Phys. Lett.*, 1985, **115**, 454.
10 B. N. Figgis, J. B. Forsyth, and P. A. Reynolds, *Inorg. Chem.*, 1987, **26**, 101.
11 F. A. Wedgewood, *Proc. R. Soc. (London), Ser. A*, 1976, **249**, 447.
12. B. N. Figgis, P. A. Reynolds, and G. A. Williams, *J. Chem. Soc., Dalton Trans.*, 1980, 2348.
13 W. G. Palmer, 'Experimental Inorganic Chemistry,' Cambridge University Press, 1954, p. 413.
14 B. N. Figgis, P. A. Reynolds, A. H. White, G. A. Williams, and S. Wright, *J. Chem. Soc., Dalton Trans.*, 1981, 997.
15 J. M. Stewart and S. R. Hall (eds.), 'The XTAL System of Crystallographic Programs,' Computer Science Technical Report TR-901, 1986, University of Maryland, U.S.A.
16 'International Tables for *X*-Ray Crystallography,' Kynoch Press, Birmingham, 1974, vol. 4.
17 D. T. Cromer and D. Liberman, *J. Chem. Phys.*, 1970, **53**, 1891.
18 E. Clementi and C. Roetti, 'Atomic Data and Nuclear Data Tables,' 1974, **14**, 177.
19 B. N. Figgis and P. A. Reynolds, *Inorg. Chem.*, 1985, **24**, 1864.
20 A. D. McLean and M. Yoshimine, 'Tables of Linear Molecule Wavefunctions,' I.B.M., San Jose, California, 1967.
21 B. N. Figgis, E. S. Kucharski, and P. A. Reynolds, *J. Am. Chem. Soc.*, 1989, **111**, 1683.

Received 1*st November* 1988; *Paper* 8/04349C